



AUTHOR(S):

TITLE:

YEAR:

Publisher citation:

OpenAIR citation:

Publisher copyright statement:

This is the _____ version of proceedings originally published by _____
and presented at _____
(ISBN _____; eISBN _____; ISSN _____).

OpenAIR takedown statement:

Section 6 of the "Repository policy for OpenAIR @ RGU" (available from <http://www.rgu.ac.uk/staff-and-current-students/library/library-policies/repository-policies>) provides guidance on the criteria under which RGU will consider withdrawing material from OpenAIR. If you believe that this item is subject to any of these criteria, or for any other reason should not be held on OpenAIR, then please contact openair-help@rgu.ac.uk with the details of the item and the nature of your complaint.

This publication is distributed under a CC _____ license.

Insulating Polymer Nanocomposites for High Thermal Conduction and Fire Retarding Applications

Ranjeetkumar Gupta¹, Dehong Huo², Mehul Pancholi³, James Njuguna¹, Ketan Pancholi^{1,*}

¹ School of Engineering, Robert Gordon University, Aberdeen, UK.

² School of Mechanical and System Engineering, Newcastle University, Newcastle upon Tyne, UK.

³ Technology and Innovation, Linde Group, Guildford, UK.

* k.pancholi2@rgu.ac.uk

Abstract. The possibility of combining the flexibility and light-weight of polymers with the highest insulation of ceramics, drives the field of nanocomposites for potential commercial application. The inclusion of nano-sized insulating particles in the polymer matrix, and orienting the fillers along the direction of heat flow results in modifying the induced interfaces for effective phonon propagation. Such flexible polymer nanocomposites (PNC) offer easy workability and refined insulating effect with high thermal conductivity and fire-retardancy. Hence, opening a wider arena of applications with the advantage of their light-weight. The engineering of the interfaces, is the key for dictating the desired properties at the macro-scale. Consequently, silane functionalisation of nanoparticles with designed dispersion technique was tried for achieving this purpose. Transmission electron microscopy (TEM), Fourier transform infrared (FT-IR) spectroscopy, Differential scanning calorimetry (DSC), Thermogravimetric analysis (TGA), and Dynamic mechanical analysis (DMA) were done to characterize the properties and structure of the synthesised nanocomposite.

This paper reports that surface modification of the nanoparticles can effectively solve the dispersion problem and reduces the electric field charge concentration at the interface. Synthesising PNC with selective nanoparticle loading percentage can yield almost 6-12% increase in the thermal capacity and fire retardability of the base polymer. Presenting an effective way of resulting in a commercially promising PNC suitable for various defence applications of radome technology, energy storage (e.g. batteries), structural bodies and cables in general.

Keywords.

Nanocomposite, Aluminium oxide, Barium titanate, Thermal conductivity, Dielectric, Piezoelectric, Fire retardant.

1. Introduction

Polymers are by far taken as the best insulators, for various applications. Considering polymers already are light weight, easy to fabricate and chemically resistive, but if could also have increased thermal conductivity capability, then it'll have even huge application area as thermal interface materials [1]. Likewise, to improve the thermal conductivity value of polymer, various filler additives like ceramic particles [2], carbon black [3], metal powders [4], etc. have been added to the polymer matrix. Though the high thermal resistance between the inclusions and the polymer matrix, limits the enhancement of thermal conductivity [5,6]. Hence, demanding higher proportion of filler contents to fulfil a genuinely thermally conductive network; and often deteriorating the physical properties with high overall cost [7-9].

Inorganic nanoparticles (NPs) included in polymer matrix can face challenges with the discontinuous filler network, high interfacial thermal resistance, and requirement of short distance for phonon transmission. Hence, any filler to be selected is judged on its ability to form robust and continuous network with least specific surface area, alongside presenting lowest interfacial thermal resistance. Several techniques are being tested, like including enhanced thermal conductivity of polymer [10,11],

hybrid fillers [12-17], surface modification of the additives [18-21], selective distribution of fillers [22-25], controlling orientation of fillers [26], etc. Though these methods individually have still resulted in limited betterment as far as improved thermal conductivity is concerned; demanding a detailed study of them or development of a synergetic method combining benefits of multiple methods.

Regarding flame retardancy, inorganic NPs have already been used and tested in textile polymers, and are awaiting more developments for various futuristic application. The NPs can act as carrier to heat and mass transfer, limit the polymer chain mobility, and modify degradation pathway of the polymer. The increased heat transfer can tend to slow down the bubble migration, reduction in heat release and local oxygen content of the oxides via oxidation-reduction mechanisms [27,28]. Hence with inorganic NPs inclusion the improvements in flame retardant parameters is very promising.

In this paper we report a more reliable, most importantly cost-effective and scalable method for achieving high-TC and fire retarding capability in polymer nanocomposites, that can be used for various fields and in-particular for demanding defence applications.

2. Materials and Methods

A. Materials.

Polyethylene-Low Density (LDPE) granules with a melt flow rate of 2 g and density 920 kg/m^3 was received from Goodfellow (UK). Trimethoxy(octadecyl)silane of technical grade, 90%; Heptane, anhydrous, 99%; Aluminium oxide (Al_2O_3) nanopowder, less than 50 nm particle size (TEM) and; Barium titanate(IV) (BaTiO_3) nanopowder, less than 100 nm particle size (BET) with dielectric constant of 150 and density 608 kg/m^3 ; Cis-cyclooctene containing 100-200 ppm irganox 1076 FD as antioxidant, 95% were all purchased from Sigma Aldrich (UK). Other laboratory agents were used as standard.

B. Experimental Methods.

Firstly, the mixture of Al_2O_3 and BaTiO_3 in the ratio 50-50 weight % was prepared and put in the oven at $500 \text{ }^\circ\text{C}$ for 20 minutes, in order to remove any entrapped moisture content. Afterwards 2 gm of this mixture was dispersed in 600 ml of n-Heptane solvent and silane added alongside while ultrasonication at 100 kHz intensity. It was left under sonication for 30 minutes, to ensure that the NP clumps, if any, were thoroughly broken down and the particles would start the reaction for coating. Here a small sample was collected to observe the size-distribution in zeta-sizer, and the results were in the range of 60-140 nm. This can imply that the silane coating has raised the mean diameter size of the particles. After sonication, the mixture was left overnight at $25 \text{ }^\circ\text{C}$ under magnetic bar stirring for complete reaction to take place. Later next day the particles were separated under centrifuge. Centrifuging was done for 3 times on IEC Centra – 4X Centrifuge make of International Equipment Company; to eliminate any excess silane from the particle surface. It was run at 3000 rpm speed and for 8 minutes time, and using fresh solvent to clean the particles after every run. Another sample was collected here to observe the size distribution under zeta-sizer, and it yielded a satisfactory result of 100 -140 nm. The collected particles were then put in oven for drying at $1000 \text{ }^\circ\text{C}$ for 10 minutes.

The extrusion process was carried on Twin-tech 10 mm twin-screw extruder at temperatures of all the zones fixed at $140 \text{ }^\circ\text{C}$, viz. considered optimum temperature for extruding the polymer grade that we had ordered. Before extruding, the nanoparticles were mixed together with the polymer granules using 0.5 ml of cis-cyclooctene. The polymer taken was 15 gm and NPs were in 3 wt %, and the cis-cyclooctene made the NPs stick on the surfaces of the polymer granules, making a layered-coating on them. The inclusion of cis-cyclooctene was to prevent any oxygen to react with the NPs during the processing and

extrusion period. The screw speed was set to 60 rpm and the mixture was fed through the feeding hooper. After the first run the extruded sample was collected and chipped into pieces, so as to be fed again. This was done to improve the dispersionability of the NPs in the polymer melt. Same was repeated twice for effective results. Finally, the synthesised polymer nanocomposite was collected as wire samples and also in film form for further tests and characterisations.

C. Characterisation.

Transmission electron microscopy (TEM) spectroscopy was done on JEOL 1400 plus attached with AMT UltraVUE camera with accelerating voltage of 120kV; basically, to characterise the changes brought about by the silane coating on the NPs morphology and to confirm whether the same was effectively achieved.

For picking up on the bond changes of the polymer due to silane coating and the NPs inclusion itself, the Perking Elmer Attenuated Total Reflection- Fourier Transmission Infrared (ATR-FTIR) Spectrum Gx system with DGS-KBr sensor at a resolution of 4 cm⁻¹ was used.

Differential scanning calorimetry (DSC) and Thermogravimetric analysis (TGA) was performed using a TA Instruments DSC Q100 and TGA Q500 at a heating rate of 10°C/min and nitrogen cooling environment with a temperature range of 22 to 170 °C and 30 to 500 °C respectively. The main purpose of these were to study the thermal stability, or the thermal conductive behaviour of the nanocomposite and the influence of NP fillers on shifting the glass transition and subsequent thermal decomposition.

Lastly, the mechanical properties of the samples were studied by Dynamic mechanical analysis (DMA), carried out at 1 Hz frequency and 0.3 mm static displacement.

3. Results and Discussions

There are various types of silane coupling agents, and they are commonly used as grafting agents to strengthen interfacial behaviour of certain inorganic oxides, at the nanoscale, thus increasing dispersion levels of these nanoparticles when dispersed in various polymer matrix. The silanisation process initiates with a hydrolysis reaction which converts the trimethoxyl groups into trihydroxyl groups. This is then followed by a polycondensation reaction of these hydroxyl groups with the hydroxyl groups on the NPs surface.

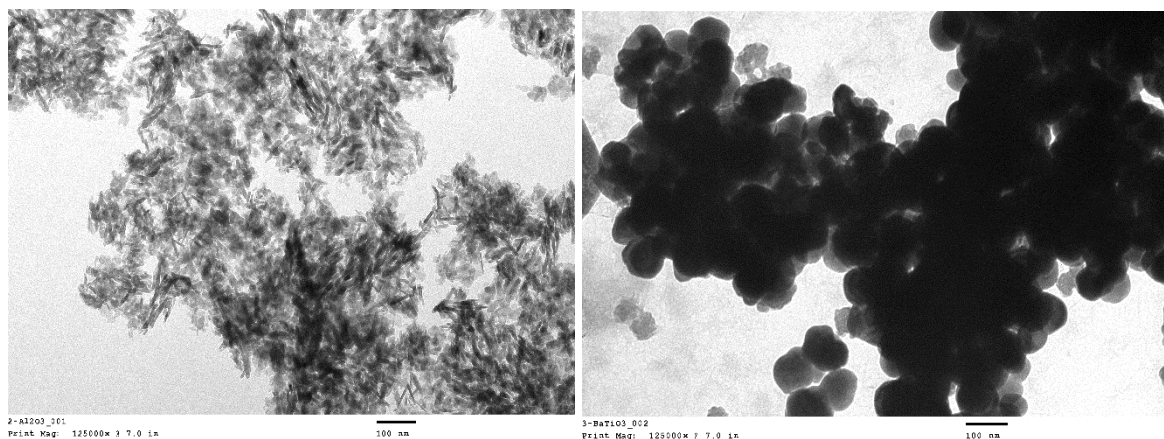


Figure 1 (a): Bare Al_2O_3 (left) and BaTiO_3 (right) nanoparticles. (Scale: 100nm)

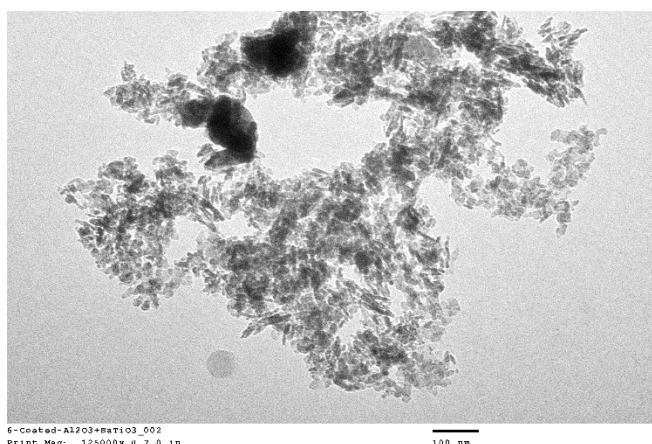


Figure 1 (b): Silane coated Al_2O_3 + BaTiO_3 nanoparticles mixture. (Scale: 100nm)

The TEM images as shown in above figure-1 (a) & (b), distinguishes the smooth surface of the uncoated NPs with that of the silane coated NPs with a faint layer of silane around. Also, in the uncoated image the particles are quite clustered together due to the dipole-dipole attraction of NPs, whereas, the coated particles are seen to be more spread out, though connected with each other but very less overlaps are seen. The images simply confirm the fact that the silane has been effectively adsorbed on the NPs surface, giving them such faint textures on the surface. Interesting observation can be seen in the aligned arrangement of the coated particles, hence hinting on the effect of the designed interfaces.

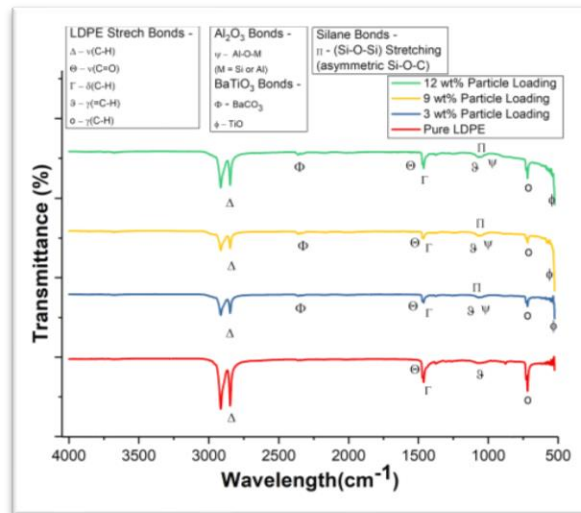


Figure 2: FT-IR spectra for different wt% of NP loading.

The FT-IR spectra investigation particularly highlights the changes due to the silane coated NPs inclusion in the base LDPE polymer matrix. Initial stretch bonds of the LDPE like the backbone stretch peak of (C-H) is seen around 1600-1800 cm^{-1} , then the other representative peaks of (C=O), $\delta(\text{C-H})$, $\nu(\text{C-H})$ and $\gamma(\text{C-H})$ is subsequently seen at around 1550 cm^{-1} , 1500 cm^{-1} , 1050 cm^{-1} and 1200 cm^{-1} respectively; though with subsequent slight shifts with increasing wt% of NP loading, as distinctive in the figure 2. These indicative peaks, though slightly suppressed at higher wt% loading, represent that the polymer backbone is effectively maintained, even with the highest wt% loading of the NP. Also, peaks for Al_2O_3 and BaTiO_3 are subsequently seen gradually increasing in size, as the wt% loading increases; hence confirming the increased NPs presence. And even the silane stretching is seen to be gradually increasing at around 1000-1100 cm^{-1} , since more NPs implies more silane coating also; though the stretching is not to drastically changing in the plot, this confirms that the particles are not overly coated, or neither there are any huge variations in silane coating between the different samples. This hint to the proportional coating volume in the different samples. Hence, the FT-IR spectra proves to be a very helpful medium to confirm and check the various functional groups and track their variations with the increase in NP wt% loading.

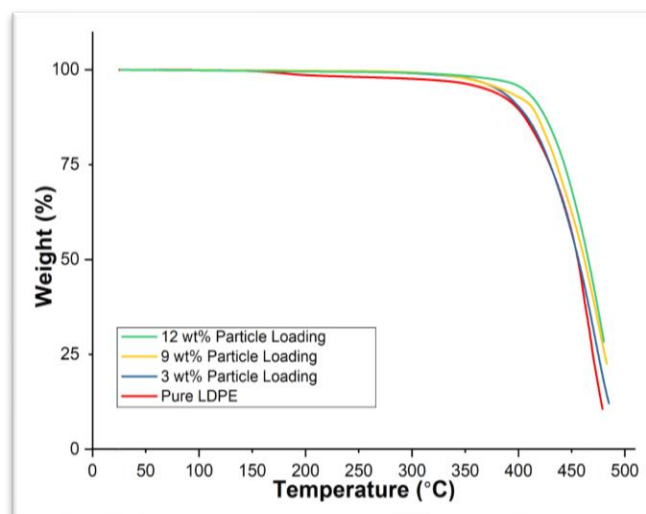


Figure 3: TGA curves for different wt% of NP loading.

To establish the relevance of the thermal stability of the composite, TGA and DSC investigation was undertaken. Firstly, from the TGA plot, as shown in figure 3, we can clearly see the effect of filler NPs on the sample decomposition. With the increasing weight proportion of NPs, there is a reduction in % weight loss, indicating that the tendency of the PNC to resist deterioration due to heat also increases. Quantitatively there is an increase of almost 9-12% (from the universal analysis software, installed to work with the setup) in the resistance to weight loss, from the virgin LDPE to the 12 wt% NP loading; as can be seen from the plot in figure 3.

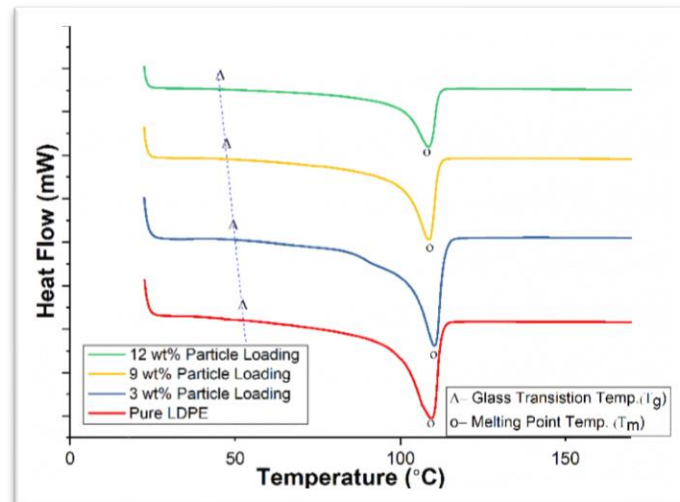


Figure 4: DSC curves for different wt% of NP loading.

Secondly, the DSC plots in figure 4 show a noticeable decline in the T_g as the NP loading increases in the PNC; as observed in earlier instances [29]. This can be attributed to the fact that increased NPs loading ease the thermal transfer, due to increased interfaces; hence decreasing the temperature gradient inside the sample. This implies the fact that the sample showing early glass transition has higher thermal conductivity compared to the one with later glass transition. There is almost a change of 6-8 % in the occurrence of the T_g in the NP loaded samples as compared to the pure LDPE sample. Hence, both the results of TGA and DSC prove our attempts successful in creating better thermally conductive and fire retarding PNC.

The dynamic mechanical results (DMA) were taken for storage modulus (E') and as plotted in figure 5. Figure 5 shows the temperature dependence of storage moduli (E') of the composites, and were found to be higher than those of the corresponding LDPE. The gradient of moduli with respect to temperature was lower. It shows that the deformation of the nanocomposite was lower at lower temperature ($<0^\circ\text{C}$) but it increased more as temperature reached above 0°C . The storage modulus E' of the nanocomposites increased with increasing the nanoparticle contents.

The polymer part of the nanocomposite consists of free macromolecular chains which is similar to that of pure polymer, however, the interphase between NPs and polymer changes due to confinement of NPs between molecular chains. Stronger the interaction more changes would occur in interphase region and volume of region would be high as well. If particles are well dispersed, the interphase region would be higher, leading to different behaviour of PNC than the pure polymer. Because of such region, the polymer deformed more than nanocomposite. Here the interphase region in nanocomposite was crystallised and prevented deformation.

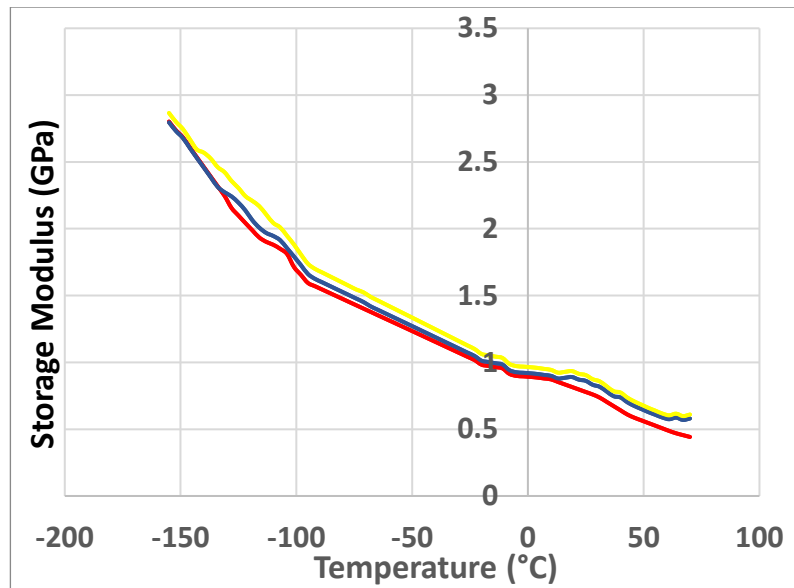


Figure 5: DMA plot for different wt% loading of NP.

4. Conclusions

This method proves our attempts successful in creating better thermally conductive and fire retarding PNC. Also, the functionalisation of NPs has improved the dispersion and subsequent filler variations have given a distinctive idea on the behaviour of the base polymer matrix. Considering the past works for similar achievements, we can note that the improvements reported in the thermal conductivity behaviour of PNC is always above 25%, but this achievement comes under a great cost, as the nano-inclusions that they used for this achievement was carbon nano-tubes (CNT) or rods or even carbon nano-platelets, which are comparably at least 20 times costlier than the ceramics that we have used in this reported work. And the main challenge is to control the effective dispersion, most importantly the alignment of CNT or platelets length along the direction of phonon propagation, without which there won't be any appreciable improvements in the conductivity of the composites. The alignment is a least concern in our case, as the NPs are spherical in shape, and the functionalisation takes care of the dispersion. Hence, the work reported here is easily scalable and very cost-effective to be brought into commercial application.

References

1. Suh, D., Moon, C.M., Kim, D. and Baik, S., 2016. Ultrahigh Thermal Conductivity of Interface Materials by Silver-Functionalized Carbon Nanotube Phonon Conduits. *Advanced Materials*, 28(33), pp.7220-7227.
2. Huang, X., Wang, S., Zhu, M., Yang, K., Jiang, P., Bando, Y., Golberg, D. and Zhi, C., 2014. Thermally conductive, electrically insulating and melt-processable polystyrene/boron nitride nanocomposites prepared by in situ reversible addition fragmentation chain transfer polymerization. *Nanotechnology*, 26(1), p.015705.
3. Agari, Y. and Uno, T., 1985. Thermal conductivity of polymer filled with carbon materials: effect of conductive particle chains on thermal conductivity. *Journal of applied polymer science*, 30(5), pp.2225-2235.
4. Mamunya, Y.P., Davydenko, V.V., Pissis, P. and Lebedev, E.V., 2002. Electrical and thermal conductivity of polymers filled with metal powders. *European polymer journal*, 38(9), pp.1887-1897.
5. Cao, J.P., Zhao, J., Zhao, X., You, F., Yu, H., Hu, G.H. and Dang, Z.M., 2013. High thermal conductivity and high electrical resistivity of poly (vinylidene fluoride)/polystyrene blends by controlling the localization of hybrid fillers. *Composites Science and Technology*, 89, pp.142-148.
6. Shen, H., Guo, J., Wang, H., Zhao, N. and Xu, J., 2015. Bioinspired modification of h-BN for high thermal conductive composite films with aligned structure. *ACS applied materials & interfaces*, 7(10), pp.5701-5708.
7. Agari, Y., Ueda, A. and Nagai, S., 1991. Thermal conductivity of a polyethylene filled with disoriented short-cut carbon fibers. *Journal of Applied Polymer Science*, 43(6), pp.1117-1124.
8. Morishita, T. and Okamoto, H., 2016. Facile exfoliation and noncovalent superacid functionalization of boron nitride nanosheets and their use for highly thermally conductive and electrically insulating polymer nanocomposites. *ACS applied materials & interfaces*, 8(40), pp.27064-27073.
9. Zhang, R.C., Sun, D., Lu, A., Askari, S., Macias-Montero, M., Joseph, P., Dixon, D., Ostrikov, K., Maguire, P. and Mariotti, D., 2016. Microplasma processed ultrathin boron nitride nanosheets for polymer nanocomposites with enhanced thermal transport performance. *ACS applied materials & interfaces*, 8(21), pp.13567-13572.
10. Yoshihara, S., Sakaguchi, M., Matsumoto, K., Tokita, M. and Watanabe, J., 2014. Influence of molecular orientation direction on the in-plane thermal conductivity of polymer/hexagonal boron nitride composites. *Journal of Applied Polymer Science*, 131(3).
11. Huang, X., Zhi, C., Jiang, P., Golberg, D., Bando, Y. and Tanaka, T., 2013. Polyhedral oligosilsesquioxane-modified boron nitride nanotube based epoxy nanocomposites: an ideal dielectric material with high thermal conductivity. *Advanced Functional Materials*, 23(14), pp.1824-1831.
12. Ma, A.J., Chen, W. and Hou, Y., 2012. Enhanced thermal conductivity of epoxy composites with MWCNTs/AIN hybrid filler. *Polymer-Plastics Technology and Engineering*, 51(15), pp.1578-1582.
13. Zhang, W.B., Zhang, Z.X., Yang, J.H., Huang, T., Zhang, N., Zheng, X.T., Wang, Y. and Zhou, Z.W., 2015. Largely enhanced thermal conductivity of poly (vinylidene fluoride)/carbon nanotube composites achieved by adding graphene oxide. *Carbon*, 90, pp.242-254.
14. Yu, A., Ramesh, P., Sun, X., Bekyarova, E., Itkis, M.E. and Haddon, R.C., 2008. Enhanced thermal conductivity in a hybrid graphite nanoplatelet-carbon nanotube filler for epoxy composites. *Advanced Materials*, 20(24), pp.4740-4744.
15. Zhou, T., Wang, X., Liu, X. and Xiong, D., 2010. Improved thermal conductivity of epoxy composites using a hybrid multi-walled carbon nanotube/micro-SiC filler. *Carbon*, 48(4), pp.1171-1176.
16. Im, H. and Kim, J., 2012. Thermal conductivity of a graphene oxide-carbon nanotube hybrid/epoxy composite. *Carbon*, 50(15), pp.5429-5440.
17. Lee, S.H., Jung, J.H. and Oh, I.K., 2014. 3D Networked Graphene-Ferromagnetic Hybrids for Fast Shape Memory Polymers with Enhanced Mechanical Stiffness and Thermal Conductivity. *Small*, 10(19), pp.3880-3886.

18. Gu, J., Guo, Y., Lv, Z., Geng, W. and Zhang, Q., 2015. Highly thermally conductive POSS-g-SiCp/UHMWPE composites with excellent dielectric properties and thermal stabilities. *Composites Part A: Applied Science and Manufacturing*, 78, pp.95-101.
19. Zhang, X., Wu, H. and Guo, S., 2015. Effect of interfacial interaction on morphology and properties of polyethylene/boron nitride thermally conductive composites. *Polymer-Plastics Technology and Engineering*, 54(11), pp.1097-1105.
20. Shen, H., Guo, J., Wang, H., Zhao, N. and Xu, J., 2015. Bioinspired modification of h-BN for high thermal conductive composite films with aligned structure. *ACS applied materials & interfaces*, 7(10), pp.5701-5708.
21. Huang, X., Zhi, C., Jiang, P., Golberg, D., Bando, Y. and Tanaka, T., 2013. Polyhedral oligosilsesquioxane-modified boron nitride nanotube based epoxy nanocomposites: an ideal dielectric material with high thermal conductivity. *Advanced Functional Materials*, 23(14), pp.1824-1831.
22. Cao, J.P., Zhao, J., Zhao, X., You, F., Yu, H., Hu, G.H. and Dang, Z.M., 2013. High thermal conductivity and high electrical resistivity of poly (vinylidene fluoride)/polystyrene blends by controlling the localization of hybrid fillers. *Composites Science and Technology*, 89, pp.142-148.
23. Cao, J.P., Zhao, X., Zhao, J., Zha, J.W., Hu, G.H. and Dang, Z.M., 2013. Improved thermal conductivity and flame retardancy in polystyrene/poly (vinylidene fluoride) blends by controlling selective localization and surface modification of SiC nanoparticles. *ACS applied materials & interfaces*, 5(15), pp.6915-6924.
24. Gu, J., Li, N., Tian, L., Lv, Z. and Zhang, Q., 2015. High thermal conductivity graphite nanoplatelet/UHMWPE nanocomposites. *RSC Advances*, 5(46), pp.36334-36339.
25. Eksik, O., Bartolucci, S.F., Gupta, T., Fard, H., Borca-Tasciuc, T. and Koratkar, N., 2016. A novel approach to enhance the thermal conductivity of epoxy nanocomposites using graphene core-shell additives. *Carbon*, 101, pp.239-244.
26. Kuang, Z., Chen, Y., Lu, Y., Liu, L., Hu, S., Wen, S., Mao, Y. and Zhang, L., 2015. Fabrication of highly oriented hexagonal boron nitride nanosheet/elastomer nanocomposites with high thermal conductivity. *Small*, 11(14), pp.1655-1659.
27. Cinausero, N., Azema, N., Lopez-Cuesta, J.M., Cochez, M. and Ferriol, M., 2011. Synergistic effect between hydrophobic oxide nanoparticles and ammonium polyphosphate on fire properties of poly (methyl methacrylate) and polystyrene. *Polymer degradation and stability*, 96(8), pp.1445-1454.
28. Rault, F., Pleyber, E., Campagne, C., Rochery, M., Giraud, S., Bourbigot, S. and Devaux, E., 2009. Effect of manganese nanoparticles on the mechanical, thermal and fire properties of polypropylene multifilament yarn. *Polymer Degradation and Stability*, 94(6), pp.955-964.
29. Wu, H. and Kessler, M.R., 2015. Multifunctional cyanate ester nanocomposites reinforced by hexagonal boron nitride after noncovalent biomimetic functionalization. *ACS applied materials & interfaces*, 7(10), pp.5915-5926.